Targeted decay of a regulatory small RNA by an adaptor protein for RNase E and counteraction by an anti-adaptor RNA

Yvonne Göpel,[1] Kai Papenfort,[2] Birte Reichenbach,[1] Jörg Vogel,[2] and Boris Görke[1,3]

[1]Department of General Microbiology, Institute of Microbiology and Genetics, Georg-August-University, D-37077 Göttingen, Germany; [2]Institute for Molecular Infection Biology, University of Würzburg, D-97080 Würzburg, Germany

Bacterial small RNAs (sRNAs) are well established to regulate diverse cellular processes, but how they themselves are regulated is less understood. Recently, we identified a regulatory circuit wherein the GlmY and GlmZ sRNAs of *Escherichia coli* act hierarchically to activate mRNA *glmS*, which encodes glucosamine-6-phosphate (GlcN6P) synthase. Although the two sRNAs are highly similar, only GlmZ is a direct activator that base-pairs with the *glmS* mRNA, aided by protein Hfq. GlmY, however, does not bind Hfq and activates *glmS* indirectly by protecting GlmZ from RNA cleavage. This complex regulation feedback controls the levels of GlmS protein in response to its product, GlcN6P, a key metabolite in cell wall biosynthesis. Here, we reveal the molecular basis for the regulated turnover of GlmZ, identifying RapZ (RNase adaptor protein for sRNA GlmZ; formerly YhbJ) as a novel type of RNA-binding protein that recruits the major endoribonuclease RNase E to GlmZ. This involves direct interaction of RapZ with the catalytic domain of RNase E. GlmY binds RapZ through a secondary structure shared by both sRNAs and therefore acts by molecular mimicry as a specific decoy for RapZ. Thus, in analogy to regulated proteolysis, RapZ is an adaptor, and GlmY is an anti-adaptor in regulated turnover of a regulatory small RNA.

[*Keywords*: endoribonuclease RNase E; small RNA; RNA mimicry; RNase adaptor protein RapZ (YhbJ); sRNA-binding protein; glucosamine-6-phosphate synthase (GlmS)]

Supplemental material is available for this article.

Received November 12, 2012; revised version accepted January 31, 2013.

Bacterial small noncoding RNAs (sRNAs) function as regulators of gene expression in numerous diverse physiological circuits in response to changing internal or environmental cues such as metabolite concentrations or stresses (Gottesman and Storz 2011; Richards and Vanderpool 2011; Storz et al. 2011). Therefore, the activities of sRNAs must be tightly controlled, which can occur at the level of biogenesis or decay or both. In the past decade, it became evident that sRNA expression is elaborately regulated at the transcriptional level, and cognate transcriptional regulators have been identified for an increasing number of sRNA genes (Göpel et al. 2011; Chao et al. 2012; Holmqvist et al. 2012). Many global regulators, including alternative σ factors and two-component systems, use sRNAs to control target gene expression indirectly, providing further flexibility and fine-tuning in regulation (Gogol et al. 2011; Göpel and Görke 2012). In contrast, it is much less understood how sRNAs are regulated at the level of decay.

[3]**Corresponding author**
E-mail bgoerke@gwdg.de
Article is online at http://www.genesdev.org/cgi/doi/10.1101/gad.210112.112.

Key factors in sRNA degradation are the double-strand-specific endoribonuclease RNase III, the single-strand-specific endoribonuclease RNase E, and the 3′ → 5′ exoribonuclease polynucleotide phosphorylase (PNPase) (Arraiano et al. 2010; Storz et al. 2011; Vogel and Luisi 2011). RNase E provides the scaffolding core of the RNA degradosome protein complex, which also contains helicase RhlB, enolase, and PNPase. The degradosome promotes bulk RNA turnover (Gorna et al. 2012). RNase E and, less frequently, RNase III are also responsible for sRNA-mediated gene silencing through initiation of target mRNA degradation induced by base-pairing with the sRNA, which is often codegraded (Masse et al. 2003; Figueroa-Bossi et al. 2009; Caron et al. 2010; Bandyra et al. 2012). Several sRNAs are cleaved by RNase E or RNase III independent of their targets. Initial processing may facilitate further degradation of the sRNA by enzymes such as PNPase (Andrade et al. 2012) or generate mature sRNA species with higher regulatory activity as a consequence of either increased stability or increased affinity for the target mRNA (Davis and Waldor 2007; Papenfort et al. 2009; Soper et al. 2010). For microRNAs, the eukaryotic counterparts of bacterial sRNAs, protein factors have been implicated in the targeted processing and degradation

of selected microRNAs (Suzuki and Miyazono 2011; Xhemalce et al. 2012; Zisoulis et al. 2012). Whether there are also specific protein cofactors for the degradation of individual Hfq-associated sRNAs by core endoribonucleases such as RNase E is unknown. So far, only a few specific sRNA-binding proteins have been identified in bacteria (Pichon and Felden 2007).

An intriguing example of a complex sRNA-regulated circuit with many input functions is the GlmY/GlmZ sRNA cascade of *Escherichia coli*. GlmY and GlmZ are homologous sRNAs that jointly control synthesis of the metabolic enzyme glucosamine-6-phosphate (GlcN6P) synthase GlmS (Kalamorz et al. 2007; Urban et al. 2007; Reichenbach et al. 2008; Urban and Vogel 2008). GlmS catalyzes synthesis of GlcN6P, which is the key reaction of the amino sugar pathway providing precursors for assembly of the cell wall and the outer membrane. The ~207-nucleotide (nt)-long sRNA GlmZ base-pairs with an anti-Shine-Dalgarno sequence in the *glmS* mRNA, thereby promoting translation and concomitant stabilization of the mRNA. GlmZ is inactivated by processing to a shorter variant of 151 nt that lacks the *glmS* interaction site. The related 184-nt-long GlmY sRNA is also subject to processing at its 3′ end by an as yet unknown enzyme, resulting in a variant of 147 nt. Processed GlmY accumulates upon decreasing intracellular concentrations of GlcN6P and inhibits processing of GlmZ, thus activating *glmS* indirectly. Thus, GlmY and GlmZ operate hierarchically to attune *glmS* expression, thereby mediating GlcN6P homeostasis.

Genetic analysis identified YhbJ, a protein of unknown function, as an additional factor in this regulatory cascade (Kalamorz et al. 2007; Urban and Vogel 2008). YhbJ positively controls processing of GlmZ. In the absence of YhbJ, GlmZ is not processed, whereas overproduction of YhbJ increases the fraction of processed GlmZ, suggesting that YhbJ is limiting for GlmZ processing (Supplemental Fig. S1A). GlmY has no impact on GlmZ and *glmS* in an *yhbJ* mutant, suggesting that GlmY acts through YhbJ (Supplemental Fig. S1B; Reichenbach et al. 2008; Urban and Vogel 2008). The high similarity of both sRNAs in sequence and structure suggested that GlmY possibly acts by a mimicry mechanism on GlmZ, perhaps through targeting protein YhbJ.

In the present study, we provide molecular evidence that YhbJ acts as an adaptor protein, guiding processing of GlmZ. YhbJ specifically binds both sRNAs at a conserved central stem–loop. However, the ribonuclease responsible for GlmZ processing is RNase E rather than YhbJ itself. We found that YhbJ directly interacts with the catalytic domain of RNase E. In vitro, RNase E requires YhbJ for specific and rapid processing of GlmZ, while GlmY inhibits this reaction through sequestration of YhbJ. Thus, YhbJ is a novel type of sRNA-binding protein that targets GlmZ for degradation by RNase E. This process is counteracted by the decoy sRNA GlmY mediating hierarchy within the GlmY/GlmZ cascade. By analogy, this regulatory circuit bears a strong resemblance to the mechanism of controlled proteolysis, in which a regulatory protein is delivered to its degrading protease by an adaptor protein, while anti-adaptor proteins counteract this process through sequestration of the adaptor (Bougdour et al. 2008). In this scenario, YhbJ serves as an adaptor, recruiting GlmZ to RNase E, and sRNA GlmY acts as an anti-adaptor. Thus, we propose renaming YhbJ as RapZ (RNase adaptor protein for sRNA GlmZ).

Results

Unlike GlmZ, GlmY is not an Hfq-dependent small RNA and presumably acts by protein binding

Although GlmY and GlmZ are very similar sRNAs, they use different mechanisms to regulate *glmS*. GlmZ activates *glmS* through base-pairing. Many base-pairing sRNAs require the hexameric RNA chaperone Hfq for functionality, at least in Gram-negative bacteria (Vogel and Luisi 2011). Hfq facilitates annealing of cognate sRNA/mRNA pairs and stabilizes the resulting duplexes. Moreover, base-pairing sRNAs are often destabilized in *hfq* mutants, while protein-binding sRNAs do not show these properties (Urban and Vogel 2007). Recent coimmunoprecipitation experiments identified GlmZ as a sRNA associating with Hfq, whereas GlmY could not be detected in these Hfq pull-down assays (Chao et al. 2012). GlmY regulates *glmS* indirectly in a process that is likely to involve RapZ. However, GlmY does not control synthesis of RapZ, since neither absence nor overexpression of GlmY had any significant effect on the amount of RapZ (Supplemental Fig. S2). Collectively, these observations suggest that GlmY may not be an Hfq-binding base-pairing sRNA but uses a distinct molecular mechanism.

To corroborate this conclusion, we determined Hfq-binding affinities for GlmY and GlmZ in vitro and examined GlmY and GlmZ stabilities in an *hfq* mutant. *Trans*-encoded base-pairing sRNAs display high binding affinities for Hfq exhibiting K_ds in the range of 0.1–10 nM, whereas nonspecific RNAs have significantly lower affinities (Olejniczak 2011; Panja and Woodson 2012). Indeed, GlmZ was efficiently bound by purified Hfq in vitro (apparent K_d ~10 nM), while ~15-fold higher Hfq concentrations were required for binding of GlmY, indicating unspecific binding (Fig. 1A). Consistently, the amount of the full-length (i.e., base-pairing) variant of GlmZ was significantly reduced in the *hfq* mutant, whereas GlmY was not affected (Fig. 1B). These results indicate that GlmY does not act by Hfq-assisted base-pairing to prevent processing of GlmZ but might act by targeting of a protein, for which the most likely candidate is RapZ.

RapZ specifically binds small RNAs GlmY and GlmZ

To explore whether RapZ binds GlmY and perhaps also GlmZ, copurification experiments were performed. Recombinant RapZ carrying the Strep tag epitope at its N terminus was overexpressed in wild-type cells (Fig. 2A, bottom panel). Cells carrying the empty bait vector or a bait vector expressing the Strep-tagged phosphotransferase protein PtsN served as negative controls. Cell extracts were subjected to StrepTactin affinity chroma-

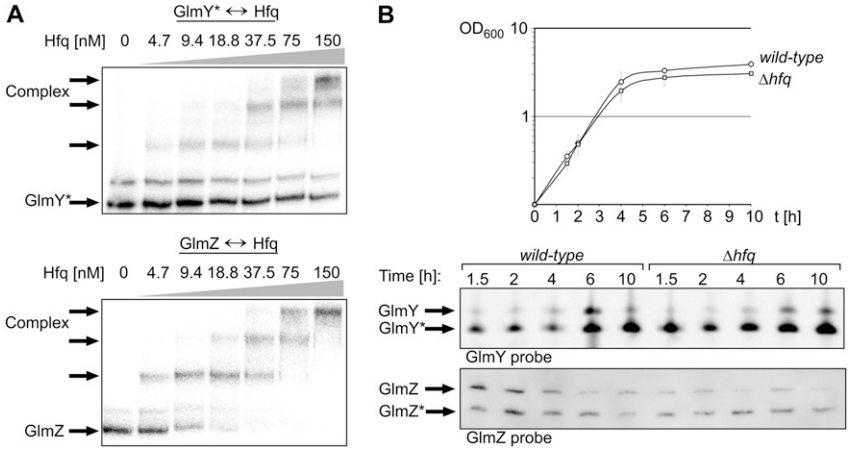

Figure 1. GlmY is not an Hfq-binding sRNA. (*A*) Hfq binds GlmZ, but not GlmY, with high affinity in vitro. Electrophoretic mobility shift assay (EMSA) using α-^{32}P-UTP-labeled GlmY (*top*) or GlmZ (*bottom*) sRNAs and various concentrations of purified Hfq as indicated. (*B*) GlmZ, but not GlmY, is destabilized in an *hfq* mutant. The processed forms of the sRNAs are marked with an asterisk in this and all other figures. (*Top*) Strain R1279 (wild-type) and the *Δhfq* mutant Z664 were grown in LB. Total RNA was isolated from samples harvested at various time intervals and analyzed by Northern blotting using the indicated probes. As loading controls, the membranes were reprobed against 5S rRNA (Supplemental Fig. S3).

tography, and recombinant proteins were eluted (Supplemental Fig. S4). Copurifying RNA was extracted from the elution fractions and analyzed by Northern blot (Fig. 2A, top panels). Notably, GlmY as well as GlmZ, both in their processed forms, were recovered with Strep-RapZ but were undetectable in the control samples. The abundant protein-binding sRNA CsrC could not be detected in any of the analyzed samples, suggesting that RapZ does not bind every sRNA.

To corroborate that RapZ binds GlmY and GlmZ specifically, the copurified RNAs were analyzed by deep sequencing (Fig. 2B). Blast analysis of the sequences of the RapZ-derived cDNA library yielded 43,644 mapped reads, 50% of which corresponded to GlmY and 30% of which corresponded to GlmZ (Fig. 2B; Supplemental Fig. S5, Supplemental Excel File S1). Thus, GlmY and GlmZ were ~1000-fold enriched by Strep-RapZ copurification as compared with the negative controls. These results demonstrated that GlmY and GlmZ are the main, if not the sole, targets of RapZ. Finally, we tested binding of GlmY and GlmZ by purified RapZ in vitro by gel retardation analysis. Both sRNAs were efficiently bound by RapZ with an apparent K_d of ~30 nM for GlmY and ~75 nM for GlmZ (Fig. 2C). Addition of unlabeled GlmY or GlmZ competitor RNA decreased complex formation. RapZ bound the full-length and the processed forms of each sRNA with similar affinity (Supplemental Fig. S6), suggesting that the 3′ ends of the sRNAs are dispensable for efficient binding. A control experiment using the unrelated sRNA MicF revealed complex formation with RapZ only at the highest protein concentrations, reflecting unspecific binding (Supplemental Fig. S7). Collectively, the results show that RapZ specifically binds GlmY and GlmZ in vivo and in vitro with high affinity. Moreover, RapZ appears to have a higher affinity for GlmY than for GlmZ.

RapZ interacts with the central stem–loops of GlmY and GlmZ, presumably via its C-terminal end

RapZ is an uncharacterized protein that shows no extended homology with other proteins; the only discernable motifs are a Walker A and a Walker B motif, which allow binding of GTP or ATP (Luciano et al. 2009). We used the software tool BindN to predict potentially RNA-binding residues in RapZ. The analysis revealed clustering of candidate residues in the C terminus of RapZ (Fig. 3A; Supplemental Material). Sequence alignment analysis of RapZ homologs from various bacteria showed that the sequence of this region is highly conserved in *Enterobacteriaceae*, which possess the GlmY/GlmZ sRNAs, but deviates in those bacteria that lack these sRNAs (Fig. 3A; Supplemental Fig. S8; Göpel et al. 2011). To determine whether the C-terminal region of RapZ is required for binding of the sRNAs, we substituted the residues K270, K281, R282, and K283 with alanine, resulting in a quadruple mutant (subsequently designated $RapZ_{quad}$) (Fig. 3A). Complementation analysis revealed that these mutations abrogated the function of RapZ in vivo. In a *ΔrapZ* mutant, unprocessed GlmZ accumulates and up-regulates *glmS* expression, as monitored by a *glmS′-lacZ* reporter fusion (Fig. 3B) and Northern blotting (Supplemental Fig. S10A). Introduction of a plasmid carrying the wild-type *rapZ* gene under control of an arabinose-inducible promoter complemented the *ΔrapZ* mutant, while this was not the case when using an isogenic construct expressing $RapZ_{quad}$ (Fig. 3B). A Western blot confirmed that the $RapZ_{quad}$ protein is expressed and stable (Supplemental Fig. S10B). Next, copurification experiments were carried out to determine whether the inactivity of $RapZ_{quad}$ in vivo is caused by an inability to bind the sRNAs. Strep-tagged $RapZ_{quad}$ and wild-type Strep-RapZ were purified by StrepTactin affinity chromatography (Supplemental Fig. S11), and copurifying RNAs were analyzed by Northern blot (Fig. 3C). Once again, GlmY and GlmZ efficiently copurified with the wild-type protein but not with the quadruple mutant. Finally, purified $RapZ_{quad}$ also failed to bind GlmY and GlmZ in gel retardation experiments (Supplemental Fig. S12). Therefore, the RapZ C terminus is required for sRNA binding, suggesting that this region is involved in RNA binding.

To determine which regions in the GlmY and GlmZ sRNAs are bound by RapZ, we performed structural

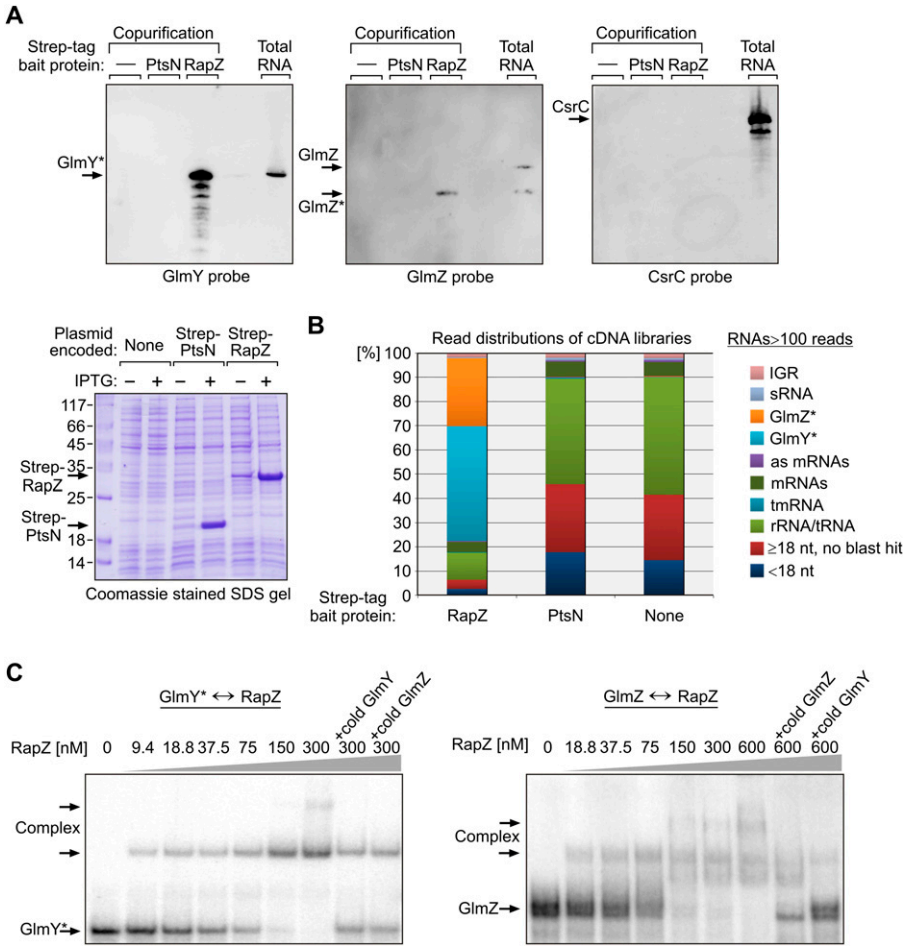

Figure 2. RapZ binds GlmY as well as GlmZ in vivo and in vitro. (*A*) GlmY and GlmZ copurify with Strep-RapZ. Transformants of strain R1279 carrying either plasmid pBGG237 (empty vector), plasmid pBGG217 encoding Strep-PtsN (molecular weight [MW] = 19.29 kDa), or plasmid pBGG164 encoding Strep-RapZ (MW = 34.04 kDa) were grown in LB, and IPTG was added to induce synthesis of recombinant proteins. (*Bottom* panel) To verify overproduction of Strep-PtsN and Strep-RapZ, total protein extracts of samples collected before and 1 h after addition of IPTG were separated on 12.5% SDS–polyacrylamide gels, and gels were analyzed by staining with Coomassie blue. The cell extracts were passed through StrepTactin columns, resulting in purification of the Strep-tagged proteins (Supplemental Fig. S4). Coeluting RNA was isolated and subjected to Northern analysis using probes specific for GlmY (*left*), GlmZ (*middle*), and CsrC (*right*). Five micrograms of total RNA of strain R1279 served as positive control (last lane, respectively). (*B*) The majority of RNA molecules copurifying with Strep-RapZ correspond to GlmY and GlmZ. The RNA preparations isolated in the copurification experiments described in *A* were converted to cDNA and analyzed by 454 pyrosequencing. The relative distribution of reads mapping to the different RNA categories is shown in 100% stacked column charts. (*C*) RapZ binds GlmY and GlmZ in vitro. EMSAs used α-^{32}P-UTP-labeled GlmY (*left*) or GlmZ (*right*) sRNAs and various concentrations of purified Strep-RapZ as indicated. In the last two lanes, 120 nM unlabeled GlmY or GlmZ corresponding to a 30-fold excess over the labeled sRNAs was added as a competitor.

probing of the sRNAs by limited RNase T1 digestion in the absence and presence of RapZ. RNase T1 cleaves ssRNA downstream from guanosine residues. The sRNAs, after 5′ end labeling with ^{32}P, were partially digested by RNase T1 in their denatured (Fig. 4A,B, lanes 3) as well as native (Fig. 4A,B, lanes 4) forms. Comparison of the cleavage patterns generated by RNase T1 generally confirmed our previous structure predictions for GlmY and GlmZ (Fig. 4C,D; Reichenbach et al. 2008; Urban and Vogel 2008). In the presence of 40 nM or 300 nM RapZ (Fig. 4A,B, lanes 5,6, respectively) several residues in GlmY and GlmZ became partially or totally protected from cleavage. These residues were located in the central stem–loop structures, in particular in the conserved lateral bulges of the sRNAs. In addition, residues in the vicinity of the processing site became protected in GlmZ. These data suggest that RapZ binds both sRNAs at similar structural motifs.

RapZ physically interacts with RNase E, which is responsible for processing of GlmZ

Previous in vivo evidence suggested that RapZ somehow triggers processing and thereby inactivation of GlmZ

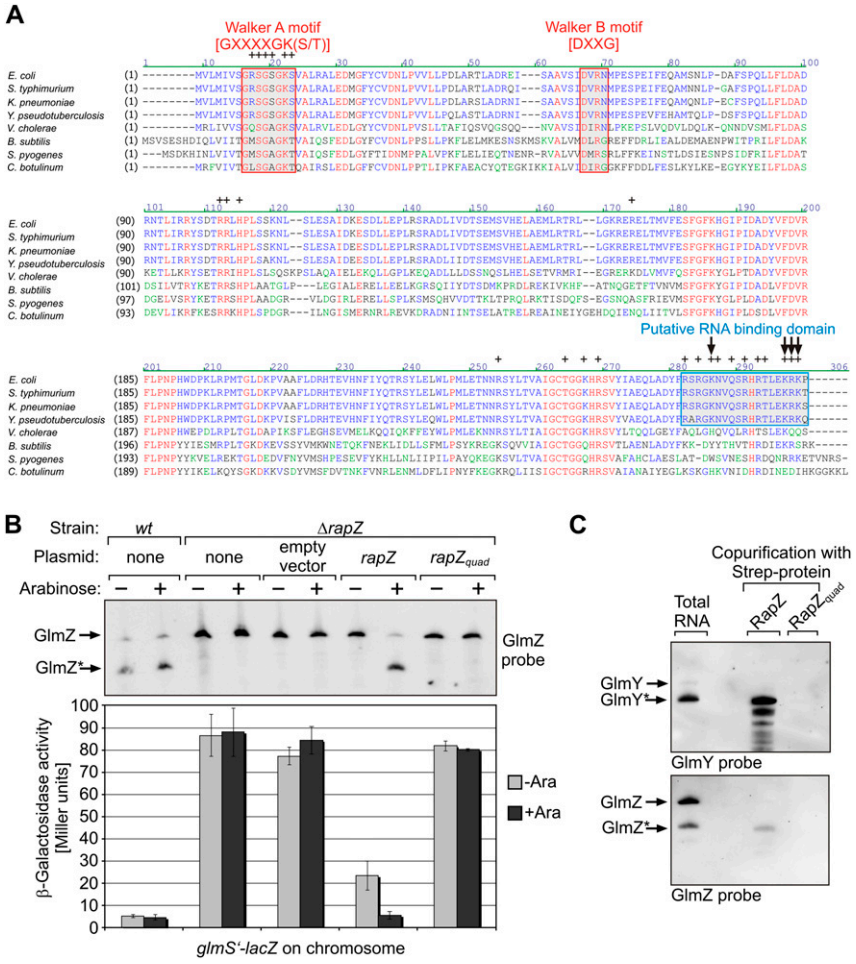

Figure 3. A RapZ variant carrying the quadruple mutation K270A–K281A–R282A–K283A in the supposed RNA-binding domain fails to bind GlmY and GlmZ. (*A*) Alignment of RapZ homologs. Putative RNA-binding amino acid residues (marked with "+") predicted by BindN cluster in the C termini of enterobacterial RapZ proteins (boxed in blue). The positions mutated in the quadruple mutant RapZ$_{quad}$ are indicated by arrows. Nucleotide-binding Walker A and B motifs are boxed in red. See the legend for Supplemental Fig. S8 for further information. (*B*) The RapZ quadruple mutant (RapZ$_{quad}$) does not complement a *ΔrapZ* mutation, as monitored by Northern blot (*top* panel) and by the expression of a *glmS′-lacZ* fusion (histogram). Strains Z8 (wild-type) and Z28 (*ΔrapZ*) were used, which carry a *glmS′-lacZ* reporter fusion on the chromosome. Additionally, transformants of strain Z28 were tested, which contained plasmids carrying either wild-type *rapZ* (plasmid pBGG61), the mutant *rapZ$_{quad}$* gene (plasmid pYG30), or no insert (empty vector pBAD33) under control of an arabinose-inducible promoter. Cells were grown in LB in the absence or presence of arabinose as indicated, and the β-galactosidase activities were determined. In addition, total RNAs were isolated and subjected to Northern blotting using a probe directed against GlmZ. The loading controls are provided in Supplemental Fig. S9. (*C*) GlmY and GlmZ do not copurify with RapZ$_{quad}$. A copurification experiment as shown in Figure 2A was carried out. Transformants of strain R1279 overproducing either Strep-RapZ$_{quad}$ (encoded on plasmid pYG29) or Strep-RapZ (encoded on plasmid pBGG164; positive control) were tested. The copurifying RNA was analyzed by Northern blot using probes specific for GlmY (*top*) or GlmZ (*bottom*). Total RNA of strain R1279 served as positive control (first lanes, respectively).

(Kalamorz et al. 2007; Urban and Vogel 2008). However, the in vitro experiments above did not yield any evidence that RapZ itself could be this processing enzyme (Figs. 2C, 4B). Therefore, we searched for ribonucleases required for processing of GlmZ. To this end, we investigated the fates of GlmY, GlmZ, and *glmS* transcripts in mutants defective for the major endoribonucleases RNase E, RNase III, and RNase G by Northern blot analysis (Fig. 5A). Since RNase E is essential, a temperature-sensitive mutant was used, which becomes nonpermissive at 44°C. While none of the RNase mutations substantially affected GlmY, processing of GlmZ was specifically inhibited upon inactivation of RNase E. As expected, this resulted in concomitant up-regulation of the *glmS* mRNA and the *glmUS* cotranscript, which undergoes processing by RNase E at the *glmU* stop codon (Joanny et al. 2007; Kalamorz et al. 2007). In conclusion, RNase E, and not RNase III as suggested previously (Argaman et al. 2001), is required for processing of GlmZ in vivo.

Next, we asked whether the stimulatory effect of RapZ on RNase E-mediated processing of GlmZ might involve a physical interaction of RapZ and RNase E. Therefore, we tested whether a chromosomally encoded RNase E-Flag variant copurified together with Strep-RapZ upon StrepTactin affinity chromatography. RNase E-Flag was indeed detectable in the elution fractions of the Strep-RapZ purification but absent from control elutions carried out with extracts of cells that expressed the Strep-PtsN protein or carried the empty bait vector (Fig. 5B; Supplemental Fig. S14). To confirm these results, bacterial two-hybrid (BACTH) assays were performed using the BACTH system, which relies on reconstitution of the activity of split adenylate cyclase CyaA in *E. coli* (Karimova et al. 1998). Indeed, high β-galactosidase activities, reflecting successful restoration of CyaA activity and therefore protein–protein interaction, were observed when RNase E and RapZ were fused to the C termini of the T25 and T18 fragments of CyaA, respectively (Fig. 5C, first column; Supplemental Fig. S15A). Comparable enzyme activities were obtained when the already established interaction of enolase and RNase E was tested as a positive control. In contrast, interaction between PtsN and RNase E (negative

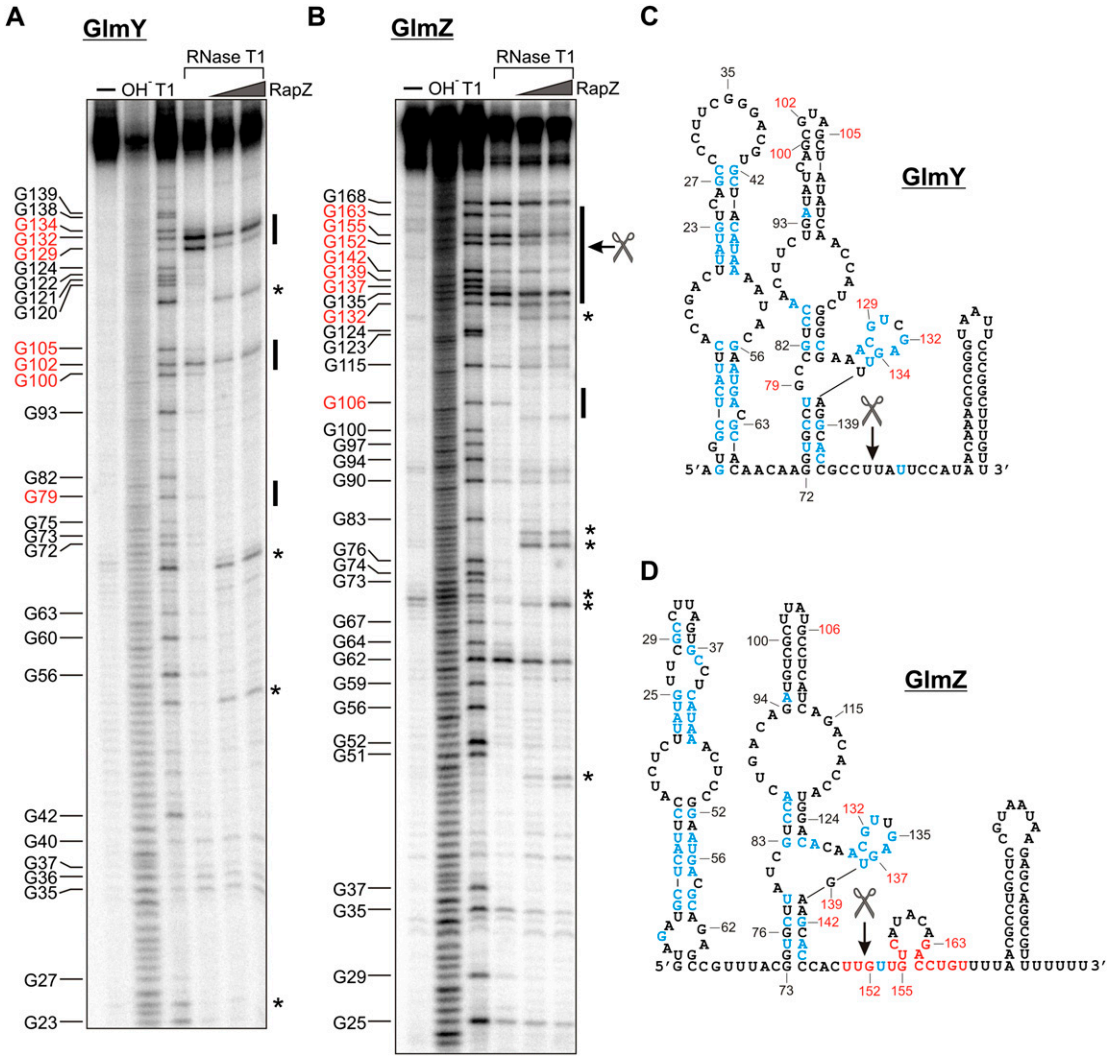

Figure 4. Identification of RapZ-binding sites in GlmY and GlmZ by RNase T1 protection assay. 5′-end-labeled GlmY (*A*) and GlmZ (*B*) sRNAs were subjected to partial RNase T1 cleavage in the absence (lanes *4*) and presence of 40 nM (lanes *5*) and 300 nM (lanes *6*) RapZ. The untreated RNAs were loaded in lanes *1*. The ladders obtained by alkali treatment were separated in lanes *2*. The RNase T1 ladders of the denatured sRNAs were separated in lanes *3*. The positions of the cleaved G residues are given at the *left* of the gels. The positions of G residues that become protected from RNase T1 cleavage by RapZ are indicated in red. Asterisks indicate unspecific cleavage. In *C* and *D*, the positions of the G residues that are protected by RapZ are depicted in the structures of GlmY and GlmZ (labeled in red). Residues labeled in blue are conserved in both GlmY and GlmZ of various enterobacterial species (Göpel et al. 2011). Processing sites are indicated by pairs of scissors. (*D*) The base-pairing residues in GlmZ are labeled in red.

control) could not be detected by the BACTH system, consistent with the results of the copurification approach (Fig. 5C, second and fourth columns). To narrow down the RapZ interaction site in RNase E, N-terminally and C-terminally truncated RNase E variants were tested in the BACTH assay (Fig. 5C, fifth to seventh columns; Supplemental Fig. S15A): RapZ preferentially interacts with the N-terminal part of RNase E (residues 1–597), which comprises its catalytic domain. However, the less-efficient interaction of RapZ with the N-terminal fragment of RNase E, as compared with the full-length protein, might indicate that residues in the RNase E C terminus also contribute to this interaction. Control experiments demonstrated the expected interaction of enolase with the C-terminal but not the N-terminal fragment of RNase E, thus verifying functionality of the T25-RNase E (499–1061) fusion protein (Supplemental Fig. S15B). In additional experiments, all interactions were tested in the opposite orientation; i.e., the various RNase E variants were fused to the CyaA-T18 domain, whereas its potential interaction partners were fused to CyaA-T25. Phenotypic monitoring of the β-galactosidase activities of the various transformants confirmed the results (Fig. 5C, right): RapZ interacts with the N-terminal part of RNase E, while enolase binds to the RNase E C terminus. To further corroborate these results, we tested interaction in vitro by dot blot far-Western analysis using purified proteins (Fig. 5D). Strep-RapZ was spotted in serial dilutions on

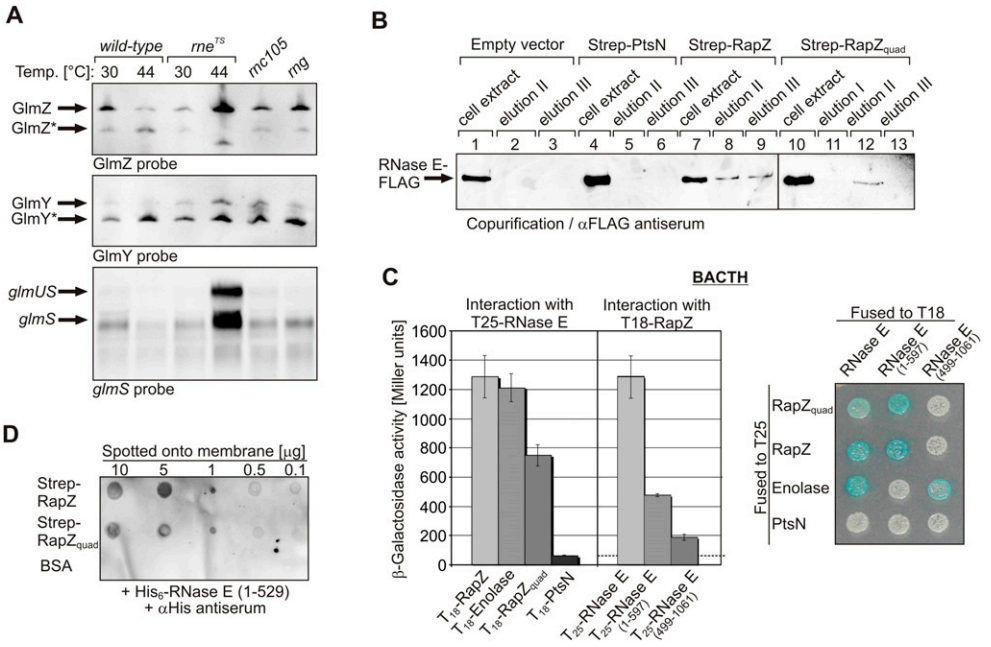

Figure 5. RapZ interacts with RNase E, which is essential for processing of GlmZ, and this interaction is independent of the RNA-binding function of RapZ. (*A*) Inactivation of RNase E abrogates processing of GlmZ in vivo. Northern blot analysis of total RNA isolated from strains N3433 (wild-type), N3431 (*rne*^{TS}), IBPC633 (*rnc*$^{-}$), and IBPC935 (*rng*$^{-}$). Strain N3431 carries a temperature-sensitive RNase E variant, which becomes inactivated upon a temperature shift from 30°C to 44°C. Northern blot analysis was performed using the indicated probes. The loading controls are provided in Supplemental Figure S13. (*B*) RNase E copurifies with RapZ independently of RNA binding by RapZ. Strain Z64, which carries a Flag-tagged *rne* gene (encoding RNase E-Flag) on the chromosome and additionally contained either plasmid pBGG237 (empty vector; lanes *1–3*), plasmid pBGG217 encoding Strep-PtsN (lanes *4–6*), plasmid pBGG164 encoding Strep-RapZ (lanes *7–9*), or plasmid pYG29 encoding Strep-RapZ$_{quad}$ (lanes *10–13*), was grown in LB containing 1 mM IPTG for induction of synthesis of the Strep-tagged proteins. The cell extracts were subjected to the copurification protocol using StrepTactin affinity chromatography (Supplemental Fig S11). The presence of RNase E-Flag in the eluates was tested by Western blotting using anti-Flag antiserum. (*C*) BACTH assays indicating interaction of the N-terminal part of RNase E with RapZ independent of its RNA-binding function. High β-galactosidase activities, which were monitored either quantitatively (*left*) or phenotypically on X-Gal agarose plates (*right*), reflect reconstitution of split adenylate cyclase CyaA activity though interaction of the proteins that are fused to its separately encoded T25 and T18 domains. The various plasmids that were tested in strain BTH101 are listed in Supplemental Table S2. (*D*) Dot blot far-Western indicating interaction of RapZ with the catalytic domain of RNase E in vitro. Various amounts of purified Strep-RapZ, Strep-RapZ$_{quad}$, and BSA (negative control) were spotted onto a membrane and subsequently incubated in 50 nM His$_6$-tagged catalytic domain of RNase E. Interaction was visualized with an antiserum directed against the His tag.

a membrane, which was subsequently incubated in a solution containing the 6xHis-tagged catalytic domain of RNase E (residues 1–529). Incubation with αHis antiserum revealed interaction of the truncated RNase E with RapZ but not with the negative controls BSA, Strep-PtsN, or RhlB (Fig. 5D; Supplemental Fig. S16). RhlB is known to interact with the C-terminal part of RNase E (Gorna et al. 2012). Essentially, the same result was obtained when the reverse experiment was carried out; i.e., when membrane-immobilized His$_6$-RNase E (1–529) was treated with a solution containing Strep-RapZ, and complexes were detected with αStrep antiserum (Supplemental Fig. S17A).

Next we analyzed whether the observed interaction between RapZ and the catalytic domain of RNase E was direct or resulted from the simultaneous interaction of both proteins with GlmZ and thus required RNA. Therefore, we tested the RapZ$_{quad}$ mutant, which lacks sRNA-binding activity (Fig. 3), in the various protein–protein interaction assays (Fig. 5B–D; Supplemental Figs. S15–S17). The data revealed that the RapZ$_{quad}$ protein still interacted with the catalytic domain of RNase E, although with a slightly decreased affinity as compared with wild-type RapZ. Together, our data suggest that RapZ directly interacts with the catalytic domain of RNase E in a RNA-independent manner.

RapZ triggers processing of GlmZ by RNase E in vitro

Our observations that RapZ interacts with GlmZ as well as with RNase E and that both proteins are required for processing of GlmZ in vivo raised the possibility that RapZ recruits GlmZ to RNase E for subsequent processing. To test this idea, processing of GlmZ by RNase E was studied in vitro. Forty nanomolar radiolabeled GlmZ were incubated with increasing concentrations of the purified catalytic domain of RNase E (Fig. 6A). This procedure did not yield significant amounts of processed GlmZ species that matched the 151-nt fragment observed in vivo (Fig. 6A–C), suggesting that RNase E alone is not

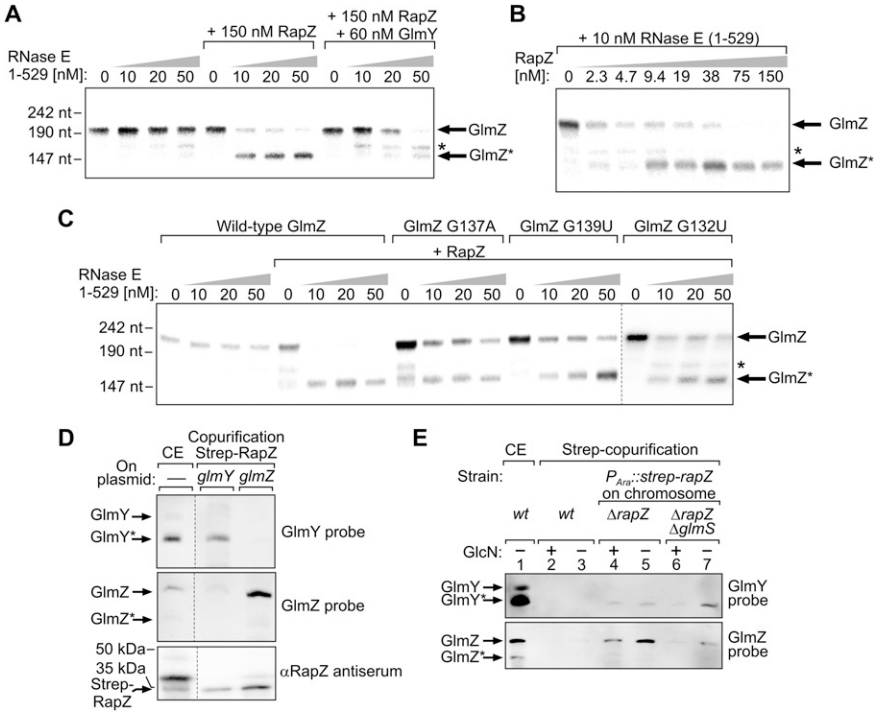

Figure 6. RapZ recruits GlmZ to processing by RNase E, and GlmY counteracts this reaction through sequestration of RapZ. (*A*) RapZ promotes cleavage of GlmZ by RNase E in vitro, and GlmY inhibits this process. In vitro cleavage assay of α-^{32}P-UTP-labeled GlmZ using varying concentrations of the catalytic domain of RNase E in the absence (lanes *1–4*) or presence (lanes *5–12*) of 150 nM Strep-RapZ. In lanes *9–12*, unlabeled GlmY (60 nM) was additionally present. The asterisk indicates a nonspecific cleavage product of GlmZ. (*B*) RapZ triggers specific processing of GlmZ. In vitro cleavage assay of α-^{32}P-UTP-labeled GlmZ using 10 nM catalytic domain of RNase E and varying concentrations of Strep-RapZ. (*C*) Mutations in the lateral bulge inhibit processing of GlmZ by RNase E in vitro. In vitro cleavage assay of α-^{32}P-UTP-labeled GlmZ variants carrying the indicated mutations. Varying concentrations of the catalytic domain of RNase E and 150 nM Strep-RapZ were added as indicated. (*D*) GlmY and GlmZ compete for binding to RapZ in vivo. The effects of plasmid-driven overexpression of GlmY and GlmZ on sRNA copurification with Strep-RapZ were addressed. Strain Z479, which carried the arabinose-inducible *strep-rapZ* gene on the chromosome and either plasmid pYG23 for overexpression of *glmY* or plasmid pYG24 for overexpression of *glmZ* was grown in LB containing arabinose. (*Bottom* panel) The cell extracts were subjected to the copurification protocol using StrepTactin affinity chromatography, resulting in purification of Strep-RapZ (Western blot). (*Top* and *middle* panels) Coeluting RNA was subjected to Northern analysis. Five micrograms of total RNA of strain Z479 served as positive control (first lanes, respectively). The dotted line indicates cropping of lanes from the original blot. (*E*) Intracellular GlcN6P depletion in a *glmS* mutant shifts the proportion of the two sRNA that are bound to Strep-RapZ toward GlmY. Strains Z479 (lanes *4*,*5*) and the isogenic Δ*glmS* mutant Z555 (lanes *6*,*7*) lack the authentic *rapZ* gene but carry the arabinose-inducible *strep-rapZ* gene at an ectopic site. The strains were grown in LB containing GlcN and arabinose until an OD_{600} = 0.3. Subsequently, the cultures were split, and growth was continued in the absence or presence of GlcN (Supplemental Fig. S21B). After 2 h, the cultures were subjected to the copurification protocol, resulting in purification of Strep-RapZ (Supplemental Fig. S23). The copurifying sRNAs were analyzed by Northern blotting. (Lanes *2*,*3*) Wild-type strain R1279 carrying no *strep-rapZ* served as negative control. (Lane *1*) Five micrograms of total RNA of strain R1279 served as positive control.

sufficient to mediate efficient GlmZ processing. Importantly, the presence of 150 nM purified RapZ in this assay promoted efficient processing of GlmZ to the product of expected size (Fig. 6A). Additional assays were carried out using a fixed concentration of 10 nM RNase E and varying concentrations of RapZ (Fig. 6B). These data revealed that RapZ triggered correct processing of GlmZ in a concentration-dependent manner. An approximately threefold excess of RapZ over RNase E was required to obtain complete processing of GlmZ within the reaction time. Interestingly, RapZ forms a homotrimer in solution (Resch et al. 2013), suggesting a 3:1 stoichiometry of RapZ and RNase E in the complex. Moreover, nonspecific cleavage was suppressed toward higher concentrations of RapZ.

Our experiments suggested that RapZ makes contacts with the lateral bulge in the central stem–loop of GlmZ (Fig. 4B,D). Residues G132, G137, and G139, located in this bulge, became protected from RNase T1 digestion in the presence of RapZ (Fig. 4B). To determine whether these residues are important for binding of GlmZ by RapZ and/or its processing by RNase E, we studied the effects of their individual mutations. Substitution of wild-type GlmZ with the corresponding GlmZ mutants caused strong up-regulation of *glmS* expression, as inferred from expression of a *glmS′-lacZ* reporter gene fusion and Northern blot analysis (Supplemental Fig. S18A,B). Gel retardation assays showed that the GlmZ mutants were still efficiently bound by RapZ, similar to wild-type GlmZ (Supplemental Fig. S18C). Notably, when tested in the in vitro cleavage assay, processing of the GlmZ mutants by RNase E was strongly inhibited as compared with wild-type GlmZ, which was tested in parallel (Fig. 6C). In conclusion, single mutations in the lateral bulge of GlmZ are not sufficient to abolish binding by RapZ but strongly impair processing by RNase E.

GlmY counteracts processing of GlmZ by acting as a decoy for RapZ

In vivo, GlmY counteracts processing of GlmZ. To reconstitute this antagonism with a minimal system, we

tested the effect of GlmY on processing of GlmZ by RNase E in vitro. To this end, 60 nM cold GlmY was added to the in vitro cleavage system containing radiolabeled GlmZ and RapZ and varying amounts of the catalytic domain of RNase E (Fig. 6A). Intriguingly, the presence of GlmY strongly inhibited processing of GlmZ. High RNase E concentrations led to some processing, but the majority of the emerging products corresponded to unspecific cleavage similar to the one observed when RapZ concentrations were limiting. Both full-length and processed GlmY inhibited cleavage of GlmZ in these in vitro assays with comparable efficiency (cf. Fig. 6A and Supplemental Fig. S19). This is consistent with our observation that RapZ binds both forms of GlmY with similar affinities in vitro (Supplemental Fig. S6A). Addition of 60 nM noncognate sRNA SraC to the in vitro cleavage system did not impair processing of GlmZ, demonstrating that this is a specific function of GlmY (Supplemental Fig. S20). These results, together with the observation that GlmY binds RapZ with high affinity (Fig. 2), indicated that GlmY counteracts processing of GlmZ through sequestration of its processing cofactor, RapZ.

To obtain in vivo evidence that GlmY and GlmZ compete for binding of RapZ, we carried out copurification experiments using Strep-RapZ as bait. To obtain physiological concentrations of RapZ, a strain was used in which the native *rapZ* gene was replaced by *strep-rapZ*, which was expressed from an arabinose-inducible promoter at the ectopic chromosomal λ*attB* site (Supplemental Fig. S21A). Control experiments verified that upon induction, Strep-RapZ triggered processing of GlmZ with the same rate as observed in the wild-type strain (Supplemental Fig. S21A). To investigate whether high concentrations of one sRNA may prevent binding of the other sRNA to RapZ, plasmids overexpressing either GlmY or GlmZ were introduced into this strain in addition to the chromosomally encoded sRNAs. Overexpression of GlmY and, to a marginally lower extent, GlmZ led to up-regulation of the *glmS* transcript (Supplemental Fig. S22), which is in agreement with previous data (Reichenbach et al. 2008; Urban and Vogel 2008). From these strains, Strep-RapZ was purified by affinity chromatography, and copurifying sRNAs were analyzed by Northern blotting (Fig. 6D). Only GlmY, not GlmZ, copurified with Strep-RapZ when the strain overexpressing *glmY* was examined. The opposite result was obtained when the strain overexpressing *glmZ* was subjected to the copurification experiment. These results showed that high concentrations of GlmY displace GlmZ from RapZ, and vice versa.

In wild-type cells, GlmY accumulates upon depletion of the cellular GlcN6P pool, which leads to the inhibition of GlmZ processing (Reichenbach et al. 2008). Therefore, we predicted that under conditions of low GlcN6P concentrations, the ratio of GlmY/GlmZ bound to RapZ should shift in favor of GlmY. To achieve GlcN6P depletion, a Δ*glmS* mutant was used. This mutant requires exogenous supplementation with amino sugars such as GlcN for viability. Upon uptake, GlcN is converted to GlcN6P, thereby bypassing the need for GlmS (Plumbridge and Vimr 1999). Withdrawal of GlcN from the culture results in cessation of growth and, finally, cell death (Supplemental Fig. S21B). Concomitantly, both sRNAs strongly accumulate; i.e., cells try to compensate for the GlcN6P downshift through activation of the GlmYZ cascade (Supplemental Fig. S21B; Reichenbach et al. 2008). Ultimately, this leads to up-regulation of a plasmid-encoded *glmS′-lacZ* fusion when present in these strains (Supplemental Fig. S21C), demonstrating induction of the complete GmY/GlmZ/*glmS* regulatory cascade upon GlcN6P depletion. The GlcN6P downshift had no significant effect on cellular RapZ levels (Supplemental Fig. S21D). Two hours after amino sugar withdrawal (Supplemental Fig. S21B), cells were harvested, and the sRNAs copurifying with the chromosomally encoded Strep-RapZ protein (Supplemental Fig. S23) were isolated and analyzed by Northern blot (Fig. 6E). Indeed, more GlmY was bound to RapZ in the GlcN-starved *glmS* mutant as compared with the isogenic *glmS*$^+$ strain (Fig. 6E, top panel, lanes 5,7). Intriguingly, the opposite pattern was observed for GlmZ (Fig. 6 E, bottom panel, lanes 5,7). Collectively, the data suggest that accumulation of GlmY, as a consequence of either its artificial overexpression or GlcN6P depletion, sequesters RapZ, leading to the displacement of GlmZ. Consequently, GlmZ is not recruited to processing by RNase E and accumulates to activate *glmS* expression (Fig. 7).

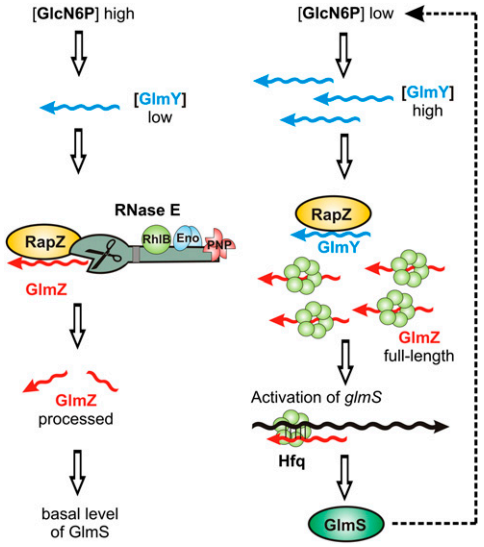

Figure 7. Model for the control of the regulatory GlmY/GlmZ cascade by RapZ. When GlcN6P concentrations are high in the cell, GlmY is present in low amounts. Under these conditions, RapZ is free to bind GlmZ and recruit it to processing by RNase E through protein–protein interaction. Consequently, GlmZ is inactivated and unable to activate GlmS synthesis. When GlcN6P levels decrease, processed GlmY accumulates and binds and sequesters RapZ. Thereby, GlmZ remains unbound and cannot be processed by RNase E. As a result, GlmZ base-pairs with *glmS* in an Hfq-dependent manner and activates synthesis of GlmS, which resynthesizes GlcN6P.

Discussion

In the present study, we provide mechanistic insight into the GlmY/GlmZ sRNA cascade regulating synthesis of the metabolic enzyme GlmS. We show that protein RapZ is a novel type of an RNA-binding adapter protein that binds sRNA GlmZ and targets it to processing by RNase E. Notably, this process involves direct interaction of RapZ with the N-terminal catalytic domain of RNase E. Cleavage of GlmZ by RNase E removes the base-pairing nucleotides and thereby inactivates the sRNA (Fig. 7, left). The homologous sRNA GlmY counteracts this process by acting as decoy sRNA for RapZ and thus functions as an anti-adaptor. GlmY accumulates upon GlcN6P depletion and sequesters RapZ. As a result, full-length GlmZ is stabilized and activates GlmS synthesis through Hfq-assisted base-pairing with its mRNA (Fig. 7, right). Thus, *E. coli* uses a regulatory circuit composed of a base-pairing sRNA, an adaptor protein, and an anti-adaptor sRNA to achieve GlcN6P homeostasis. This mechanism likely applies to all species of *Enterobacteriaceae*, in which all components of the circuit are conserved (Supplemental Fig. S8; Göpel et al. 2011).

Our work has two major implications for bacterial sRNA-mediated regulation and control of RNA turnover in general. First, proteins that selectively associate with particular sRNAs to alter their functionality might be more common in bacteria than previously thought. Second, proteins can play a major role in programming a particular RNA to processing or degradation, thus explaining how specificity in substrate recognition by RNases can be achieved.

Reconstitution of specific processing of GlmZ by RNase E in vitro required protein RapZ (Fig. 6 A,B). Thus, GlmZ per se is not an appropriate substrate for RNase E. How RNase E recognizes its various substrates has yet to be understood. In functional analogy to decapping of eukaryotic mRNAs, many RNAs require dephosphorylation at their 5′ end to initiate RNase E-mediated decay (Deana et al. 2008). Interaction with the 5′ monophosphate end of the RNA was shown to activate the catalytic function of RNase E (Callaghan et al. 2005). In the in vitro cleavage experiments (Fig. 6) GlmZ carried a triphosphate at its 5′ end. Therefore, it seems unlikely that RapZ acts by providing access for RNase E to the 5′ end of GlmZ, which is sequestered in a stable stem–loop structure (Fig. 4). This is further supported by data indicating that RapZ contacts the lateral bulge in the central stem–loop in GlmZ (Fig. 4). However, mutations in this structure were not sufficient to abolish RapZ binding (Supplemental Fig. S18); instead, they strongly impaired processing by RNase E (Fig. 6C). Thus, GlmZ might belong to the class of substrates that are recognized by RNase E through their fold and are cleaved regardless of their 5′ phosphorylation status (Kime et al. 2010; Bouvier and Carpousis 2011). It is worth noting that only processed GlmZ copurified with RapZ when RapZ was overexpressed (Fig. 2 A,B). In contrast, only full-length GlmZ copurified when RapZ was expressed at physiological concentrations (Fig. 6 D,E). In vitro RapZ binds both forms of GlmZ with similar affinities (Supplemental Fig. S6B). In vivo, RapZ might preferably bind the more abundant of both forms. In principle, this could provide the basis of a feedback mechanism inhibiting processing of GlmZ when the level of processed GlmZ exceeds a threshold that remains to be determined.

Different experimental approaches demonstrated interaction of RapZ with the N-terminal domain of RNase E, and this interaction is most likely direct (Fig. 5 B–D; Supplemental Figs. S15–S17). Thus, two different scenarios can be envisioned for the mode of action of RapZ, which remains to be explored. In the first model, RapZ might allosterically activate RNase E upon interaction, and binding of GlmZ by RapZ would serve to deliver GlmZ to RNase E located at the membrane. Upon contact, GlmZ would be released from RapZ and transferred to RNase E. In the second model, binding of RapZ would induce and stabilize structural rearrangements in GlmZ, converting it to a substrate that is recognized by RNase E. There is accumulating evidence that RNase E undergoes multiple, possibly dynamic interactions with other proteins beyond its role in the canonical RNA degradosome. For instance, an alternative degradosome containing Hfq rather than RhlB appears to degrade certain sRNAs/target mRNA duplexes (Ikeda et al. 2011). Protein CsrD was shown to selectively bind sRNAs CsrB and CsrC to promote their degradation by RNase E, but whether this involves interaction with RNase E is unknown (Suzuki et al. 2006). Recently, the RNA-binding protein RHON1 was shown to target certain plastid transcripts to processing by RNase E in *Arabidopsis* (Stoppel et al. 2012). As observed here for RapZ, this process likely involves interaction of RHON1 with RNase E. Therefore, it is tempting to speculate that RNA adaptor proteins are ubiquitously used to program ribonucleases for target specificity.

We also clarified how the sRNA GlmY counteracts processing of its homolog, GlmZ, and thereby controls *glmS* expression indirectly. In contrast to GlmZ, GlmY appears not to be a base-pairing sRNA, as it is stable in an *hfq* mutant and is bound by Hfq only with low affinity (Fig. 1). Given the high similarity of both sRNAs, this difference is remarkable. According to recent reports, an accessible poly(U) tail appears to be critical for sRNA binding to Hfq (Otaka et al. 2011; Sauer and Weichenrieder 2011). The poly(U) tail of GlmY, in contrast to that of GlmZ, is buried in a stem–loop structure, which may explain the differences in Hfq binding. Consistently, GlmY acts on *glmS* not by base-pairing, but by targeting protein RapZ. RapZ appears to recognize similar structures in both sRNAs (i.e., the central stem–loops, including the lateral bulges) (Fig. 4), presumably through a domain located at its C terminus (Fig. 3). Both sRNAs compete for binding to RapZ (Figs. 2, 6D) and GlmY outcompetes GlmZ when it accumulates as consequence of intracellular GlcN6P depletion (Fig. 6E; Supplemental Fig. S21B). Finally, GlmY prevents the RapZ-mediated processing of GlmZ by RNase E in vitro (Fig. 6A), reflecting the in vivo scenario (Reichenbach et al. 2008; Urban and Vogel 2008). In vitro, processed as well as

unprocessed GlmY are able to counteract processing of GlmZ (Fig. 6A; Supplemental Fig. S19). However, in vivo, it is processed GlmY that accumulates upon GlcN6P depletion and is responsible for inhibition of GlmZ cleavage (Supplemental Fig. S21B). In conclusion, a small RNA acts as a decoy to inhibit degradation of a second sRNA through sequestration of an RNase-recruiting protein.

The regulatory circuit investigated here strongly resembles the principle of controlled proteolysis of regulatory proteins in bacteria (Bougdour et al. 2008). In this process, a regulatory protein is recruited to the degrading protease complex through interaction with an adaptor protein. This can be counteracted by an anti-adaptor protein that binds and sequesters the adaptor, leading to stabilization of the regulator. The GlmYZ system works similarly, but here the adaptor protein targets a sRNA regulator to programmed decay and is antagonized by a sRNA anti-adapter. Such a sophisticated regulatory cascade provides multiple points of entry and exit for interaction and communication with additional molecules. For instance, usage of multiple anti-adaptor proteins allows the cell to activate the regulatory protein in response to different environmental cues (Bougdour et al. 2008). Whether similar scenarios hold true for the GlmYZ system remains to be explored.

Materials and methods

Growth conditions, plasmids, and strains

Plasmids, strains, and culture conditions are described in the Supplemental Material.

Western blotting and dot blot far-Western analysis

Western blotting and dot blot far-Western analysis were carried out as described previously (Lüttmann et al. 2012). For dot blot far-Western analysis, Strep-RapZ and Strep-RapZ$_{quad}$ were purified from strain Z106, which lacks GlmY and GlmZ. Polyclonal rabbit antisera were used at dilutions of 1:5000 (anti-RapZ, Seqlab), 1:10,000 (anti-Flag, Sigma-Aldrich), and 1:20,000 (anti-Strep, PromoKine; and anti-His, Antibodies-online.com). The antibodies were visualized with alkaline phosphatase-conjugated goat anti-rabbit IgG secondary antibodies (Promega) diluted 1:100,000 and the CDP* detection system (Roche Diagnostics).

Isolation of total RNA and Northern analysis

Purification of total RNA and Northern blotting was performed as described previously (Reichenbach et al. 2008, 2009). Digoxigenin-labeled RNA probes were produced by in vitro transcription of PCR products. Oligonucleotides BG709 and BG710 were used to generate the *csrC*-specific PCR product.

Protein purification

The purification of recombinant Strep- and His$_6$-tagged proteins is described in the Supplemental Material.

Electrophoretic mobility shift assays (EMSAs)

EMSA experiments were performed essentially as described previously (Sittka et al. 2007) using α-^{32}P-UTP-labeled RNAs, which were generated as described in the Supplemental Material. Briefly, ~4 nM heat-denatured labeled sRNA, 1 μg of yeast tRNA, and various amounts of Hfq or Strep-RapZ were incubated in 1× structure buffer (10 mM Tris at pH 7, 100 mM KCl, 10 mM $MgCl_2$) in a final volume of 10 μL for 30 min at 30°C. Protein dilutions were prepared in 1× structure buffer, and protein concentrations were calculated for RapZ monomers and Hfq hexamers, respectively. Prior to loading, 2 μL of loading buffer (50% glycerol, 0.5× TBE, 0.2% bromophenol blue) was added, and samples were subsequently separated by gel electrophoresis (8% polyacrylamide, 1× TBE) in 0.5× TBE buffer at 300 V for 3 h at 4°C. Dried gels were analyzed by PhosphorImaging.

RNA and protein copurification

Copurification experiments were carried out as described previously (Lüttmann et al. 2012). Briefly, Strep-tagged bait proteins were purified from *E. coli* cells by StrepTactin affinity chromatography. Successful purification of the bait proteins was confirmed by SDS-PAGE and subsequent analysis of the gels by staining with Coomassie blue (Supplemental Figs. S4, S8, S11) or by Western blotting using anti-RapZ antiserum (Fig. 6D; Supplemental Fig. S15). Copurifying RNase E-3xFlag was detected by Western blotting using anti-Flag antiserum. For isolation of copurifying RNAs, 300 μL of the elution fractions was extracted with phenol:chloroform:isoamyl-alcohol (25:24:1), and the RNA was precipitated with EtOH:LiCl (30:1) and resolved in 30 μL of RNase-free water. Of these samples, 2.5 μL was subjected to Northern blotting and 15 μL was used for conversion to cDNA.

Preparation of cDNA and 454 pyrosequencing

cDNA library construction and 454 pyrosequencing were performed as described for the identification of eukaryotic microRNA (Berezikov et al. 2006) but omitting size fractionation of RNA prior to cDNA synthesis (Sittka et al. 2008). The cDNAs were PCR-amplified to 20–30 ng/μL. The resulting cDNA libraries were sequenced on a Roche FLX Titanium 454 sequencer. The sequences of cDNA inserts ≥18 nt were blasted against the *E. coli* K12 genome (NC_000913). The Integrated Genome Browser software from Affymetrix was used for visualization of the location of blast hits and calculation of mapped reads per nucleotide.

β-Galactosidase assays

Overnight cultures of *E. coli* were inoculated into fresh LB medium to an OD_{600} of 0.1 and grown to an OD_{600} of 0.5–0.8. Subsequently, the cells were harvested, and the β-galactosidase activities were determined as described previously (Miller 1972). The presented values are the average of at least three measurements using independent cultures from at least two independent transformants.

RNase T1 protection assays

RNase T1 protection assays were carried out in 10-μL reactions as described previously (Sharma et al. 2007). Briefly, 0.4 pmol of the sRNA, which was 5′-end-labeled as described in the Supplemental Material, was denatured (1 min at 95°C) and chilled for 5 min on ice. Subsequently, 10× structure buffer (100 mM Tris-HCl, 1 M KCl, 100 mM $MgCl_2$ at pH 7.0), 1 μg of yeast tRNA, and, optionally, 40 nM or 300 nM Strep-RapZ were added. After incubation for 10 min at 30°C, the reaction was started by addition of 0.1 U of RNase T1 (Ambion). Following 2 min of incubation at 37°C, the reaction was stopped by addition of 100 μL of stop solution (50 mM Tris, 10 mM EDTA, 0.1% SDS at pH 8.0).

The solution was extracted with phenol:chloroform:isoamylalcohol (25:24:1), and the RNA was precipitated with ethanol:sodium acetate (pH 5.2) (30:1) and finally dissolved in 22 μL of 2× RNA loading buffer (95% formamide, 18 mM EDTA, 0.025% SDS, 0.01% Xylene cyanol, 0.01% Bromophenol blue). OH ladders were obtained by incubation of 0.8 pmol of 5′-end-labeled sRNA for 5 min in alkaline hydrolysis buffer (Ambion) at 95°C. RNase T1 ladders were generated by incubating 0.8 pmol of 5′-end-labeled sRNA in 1× sequencing buffer (Ambion) for 1 min at 95°C and subsequent addition of 0.1 U of RNase T1 and incubation for 5 min at 37°C. Reactions were stopped with 12 μL of 2× RNA loading dye. All samples were denatured for 1 min at 95°C and chilled on ice prior to loading on 6% polyacrylamide/7 M urea sequencing gels. Electrophoresis was carried out in 1× TBE at 40 W for ~2 h. The gels were dried and analyzed by PhosphorImaging.

BACTH assays

To assess protein–protein interaction in living *E. coli* cells, the BACTH system was used as described previously (Karimova et al. 1998). Details are provided in the Supplemental Material.

RNase E in vitro cleavage assay

Forty nanomolar α-^{32}P-UTP-labeled GlmZ RNA was denatured by incubation for 2 min at 70°C, followed by incubation for 5 min on ice. The RNA was renatured by incubation for 5 min at 30°C in 1× reaction buffer (25 mM Tris-HCl, 50 mM NaCl, 50 mM KCl, 10 mM $MgCl_2$, 1 mM DDT at pH 7.5) containing 0.1 mg/mL yeast tRNA (Ambion) in a volume of 8 μL. Subsequently, 1 μL of 1× reaction buffer containing the indicated concentration of Strep-RapZ was added and incubation was continued for 10 min. To determine the impact of GlmY on the cleavage assay, 60 nM denatured unlabeled GlmY was added prior to renaturing of GlmZ. Cleavage was started by addition of 1 μL of 1× reaction buffer containing the indicated concentration of the catalytic domain of RNase E, followed by incubation for 20 min at 30°C. Reactions were stopped by addition of 4 U of Proteinase K (Fermentas) and PK buffer (100 mM Tris/HCl, 12.5 mM EDTA, 150 mM NaCl, 1% SDS at pH 7.5), and the samples were incubated for 10 min at 50°C to ensure degradation of RNase E. RNA loading buffer (2×) was added, and samples were separated on 7 M urea/TBE/8% polyacrylamide gels. The gels were dried and analyzed by PhosphorImaging.

Acknowledgments

We thank Sabine Lentes for excellent technical assistance, and Jörg Stülke for laboratory space. Cynthia Sharma is acknowledged for deep sequencing analysis. We are grateful to Sue Lin-Chao, Ben F. Luisi, Eliane Hajnsdorf, and Jacqueline Plumbridge for providing plasmids and strains, and Ben F. Luisi for the gift of purified RhlB protein. Falk Kalamorz is thanked for help with the preparation of RapZ antiserum, and Barbara Waldmann is thanked for construction of plasmid pBGG403. Y.G. received a fellowship of the Dorothea Schlözer Program of the Göttingen University, and B.R. was supported by a stipend of the Studienstiftung des Deutschen Volkes. This work was supported by grants of the DFG priority program SPP1258 "Sensory and Regulatory RNAs in Prokaryotes" to B.G. and J.V.

References

Andrade JM, Pobre V, Matos AM, Arraiano CM. 2012. The crucial role of PNPase in the degradation of small RNAs that are not associated with Hfq. *RNA* **18:** 844–855.

Argaman L, Hershberg R, Vogel J, Bejerano G, Wagner EG, Margalit H, Altuvia S. 2001. Novel small RNA-encoding genes in the intergenic regions of *Escherichia coli*. *Curr Biol* **11:** 941–950.

Arraiano CM, Andrade JM, Domingues S, Guinote IB, Malecki M, Matos RG, Moreira RN, Pobre V, Reis FP, Saramago M, et al. 2010. The critical role of RNA processing and degradation in the control of gene expression. *FEMS Microbiol Rev* **34:** 883–923.

Bandyra KJ, Said N, Pfeiffer V, Gorna MW, Vogel J, Luisi BF. 2012. The seed region of a small RNA drives the controlled destruction of the target mRNA by the endoribonuclease RNase E. *Mol Cell* **47:** 943–953.

Berezikov E, Thuemmler F, van Laake LW, Kondova I, Bontrop R, Cuppen E, Plasterk RH. 2006. Diversity of microRNAs in human and chimpanzee brain. *Nat Genet* **38:** 1375–1377.

Bougdour A, Cunning C, Baptiste PJ, Elliott T, Gottesman S. 2008. Multiple pathways for regulation of σ^S (RpoS) stability in *Escherichia coli* via the action of multiple anti-adaptors. *Mol Microbiol* **68:** 298–313.

Bouvier M, Carpousis AJ. 2011. A tale of two mRNA degradation pathways mediated by RNase E. *Mol Microbiol* **82:** 1305–1310.

Callaghan AJ, Marcaida MJ, Stead JA, McDowall KJ, Scott WG, Luisi BF. 2005. Structure of *Escherichia coli* RNase E catalytic domain and implications for RNA turnover. *Nature* **437:** 1187–1191.

Caron MP, Lafontaine DA, Masse E. 2010. Small RNA-mediated regulation at the level of transcript stability. *RNA Biol* **7:** 140–144.

Chao Y, Papenfort K, Reinhardt R, Sharma CM, Vogel J. 2012. An atlas of Hfq-bound transcripts reveals 3′ UTRs as a genomic reservoir of regulatory small RNAs. *EMBO J* **31:** 4005–4019.

Davis BM, Waldor MK. 2007. RNase E-dependent processing stabilizes MicX, a *Vibrio cholerae* sRNA. *Mol Microbiol* **65:** 373–385.

Deana A, Celesnik H, Belasco JG. 2008. The bacterial enzyme RppH triggers messenger RNA degradation by 5′ pyrophosphate removal. *Nature* **451:** 355–358.

Figueroa-Bossi N, Valentini M, Malleret L, Bossi L. 2009. Caught at its own game: Regulatory small RNA inactivated by an inducible transcript mimicking its target. *Genes Dev* **23:** 2004–2015.

Gogol EB, Rhodius VA, Papenfort K, Vogel J, Gross CA. 2011. Small RNAs endow a transcriptional activator with essential repressor functions for single-tier control of a global stress regulon. *Proc Natl Acad Sci* **108:** 12875–12880.

Göpel Y, Görke B. 2012. Rewiring two-component signal transduction with small RNAs. *Curr Opin Microbiol* **15:** 132–139.

Göpel Y, Lüttmann D, Heroven AK, Reichenbach B, Dersch P, Görke B. 2011. Common and divergent features in transcriptional control of the homologous small RNAs GlmY and GlmZ in *Enterobacteriaceae*. *Nucleic Acids Res* **39:** 1294–1309.

Gorna MW, Carpousis AJ, Luisi BF. 2012. From conformational chaos to robust regulation: The structure and function of the multi-enzyme RNA degradosome. *Q Rev Biophys* **45:** 105–145.

Gottesman S, Storz G. 2011. Bacterial small RNA regulators: Versatile roles and rapidly evolving variations. *Cold Spring Harb Perspect Biol* **3:** a003798.

Holmqvist E, Unoson C, Reimegard J, Wagner EG. 2012. A mixed double negative feedback loop between the sRNA MicF and the global regulator Lrp. *Mol Microbiol* **84:** 414–427.

Ikeda Y, Yagi M, Morita T, Aiba H. 2011. Hfq binding at RhlB-recognition region of RNase E is crucial for the rapid degradation of target mRNAs mediated by sRNAs in *Escherichia coli*. *Mol Microbiol* **79:** 419–432.

Joanny G, Derout J, Brechemier-Baey D, Labas V, Vinh J, Regnier P, Hajnsdorf E. 2007. Polyadenylation of a functional mRNA controls gene expression in *Escherichia coli*. *Nucleic Acids Res* **35:** 2494–2502.

Kalamorz F, Reichenbach B, März W, Rak B, Görke B. 2007. Feedback control of glucosamine-6-phosphate synthase GlmS expression depends on the small RNA GlmZ and involves the novel protein YhbJ in *Escherichia coli*. *Mol Microbiol* **65:** 1518–1533.

Karimova G, Pidoux J, Ullmann A, Ladant D. 1998. A bacterial two-hybrid system based on a reconstituted signal transduction pathway. *Proc Natl Acad Sci* **95:** 5752–5756.

Kime L, Jourdan SS, Stead JA, Hidalgo-Sastre A, McDowall KJ. 2010. Rapid cleavage of RNA by RNase E in the absence of 5′ monophosphate stimulation. *Mol Microbiol* **76:** 590–604.

Luciano J, Foulquier E, Fantino JR, Galinier A, Pompeo F. 2009. Characterization of YvcJ, a conserved P-loop-containing protein, and its implication in competence in *Bacillus subtilis*. *J Bacteriol* **191:** 1556–1564.

Lüttmann D, Göpel Y, Görke B. 2012. The phosphotransferase protein EIIA(Ntr) modulates the phosphate starvation response through interaction with histidine kinase PhoR in *Escherichia coli*. *Mol Microbiol* **86:** 96–110.

Masse E, Escorcia FE, Gottesman S. 2003. Coupled degradation of a small regulatory RNA and its mRNA targets in *Escherichia coli*. *Genes Dev* **17:** 2374–2383.

Miller J. 1972. *Experiments in molecular genetics*. Cold Spring Harbor Laboratory Press, Cold Spring Harbor, NY.

Olejniczak M. 2011. Despite similar binding to the Hfq protein regulatory RNAs widely differ in their competition performance. *Biochemistry* **50:** 4427–4440.

Otaka H, Ishikawa H, Morita T, Aiba H. 2011. PolyU tail of *rho*-independent terminator of bacterial small RNAs is essential for Hfq action. *Proc Natl Acad Sci* **108:** 13059–13064.

Panja S, Woodson SA. 2012. Hfq proximity and orientation controls RNA annealing. *Nucleic Acids Res* **40:** 8690–8697.

Papenfort K, Said N, Welsink T, Lucchini S, Hinton JC, Vogel J. 2009. Specific and pleiotropic patterns of mRNA regulation by ArcZ, a conserved, Hfq-dependent small RNA. *Mol Microbiol* **74:** 139–158.

Pichon C, Felden B. 2007. Proteins that interact with bacterial small RNA regulators. *FEMS Microbiol Rev* **31:** 614–625.

Plumbridge J, Vimr E. 1999. Convergent pathways for utilization of the amino sugars N-acetylglucosamine, N-acetylmannosamine, and N-acetylneuraminic acid by *Escherichia coli*. *J Bacteriol* **181:** 47–54.

Reichenbach B, Maes A, Kalamorz F, Hajnsdorf E, Görke B. 2008. The small RNA GlmY acts upstream of the sRNA GlmZ in the activation of *glmS* expression and is subject to regulation by polyadenylation in *Escherichia coli*. *Nucleic Acids Res* **36:** 2570–2580.

Reichenbach B, Göpel Y, Görke B. 2009. Dual control by perfectly overlapping σ^{54}- and σ^{70}- promoters adjusts small RNA GlmY expression to different environmental signals. *Mol Microbiol* **74:** 1054–1070.

Resch M, Göpel Y, Görke B, Ficner R. 2013. Crystallization and preliminary X-ray diffraction data analysis of YhbJ from *Escherichia coli*, a key protein involved in the GlmYZ sRNA regulatory cascade. *Acta Crystallogr Sect F Struct Biol Cryst Commun.* **69:** 109–114.

Richards GR, Vanderpool CK. 2011. Molecular call and response: The physiology of bacterial small RNAs. *Biochim Biophys Acta* **1809:** 525–531.

Sauer E, Weichenrieder O. 2011. Structural basis for RNA 3′-end recognition by Hfq. *Proc Natl Acad Sci* **108:** 13065–13070.

Sharma CM, Darfeuille F, Plantinga TH, Vogel J. 2007. A small RNA regulates multiple ABC transporter mRNAs by targeting C/A-rich elements inside and upstream of ribosome-binding sites. *Genes Dev* **21:** 2804–2817.

Sittka A, Pfeiffer V, Tedin K, Vogel J. 2007. The RNA chaperone Hfq is essential for the virulence of *Salmonella typhimurium*. *Mol Microbiol* **63:** 193–217.

Sittka A, Lucchini S, Papenfort K, Sharma CM, Rolle K, Binnewies TT, Hinton JC, Vogel J. 2008. Deep sequencing analysis of small noncoding RNA and mRNA targets of the global post-transcriptional regulator, Hfq. *PLoS Genet* **4:** e1000163.

Soper T, Mandin P, Majdalani N, Gottesman S, Woodson SA. 2010. Positive regulation by small RNAs and the role of Hfq. *Proc Natl Acad Sci* **107:** 9602–9607.

Stoppel R, Manavski N, Schein A, Schuster G, Teubner M, Schmitz-Linneweber C, Meurer J. 2012. RHON1 is a novel ribonucleic acid-binding protein that supports RNase E function in the *Arabidopsis* chloroplast. *Nucleic Acids Res* **40:** 8593–8606.

Storz G, Vogel J, Wassarman KM. 2011. Regulation by small RNAs in bacteria: Expanding frontiers. *Mol Cell* **43:** 880–891.

Suzuki HI, Miyazono K. 2011. Emerging complexity of microRNA generation cascades. *J Biochem* **149:** 15–25.

Suzuki K, Babitzke P, Kushner SR, Romeo T. 2006. Identification of a novel regulatory protein (CsrD) that targets the global regulatory RNAs CsrB and CsrC for degradation by RNase E. *Genes Dev* **20:** 2605–2617.

Urban JH, Vogel J. 2007. Translational control and target recognition by *Escherichia coli* small RNAs *in vivo*. *Nucleic Acids Res* **35:** 1018–1037.

Urban JH, Vogel J. 2008. Two seemingly homologous noncoding RNAs act hierarchically to activate *glmS* mRNA translation. *PLoS Biol* **6:** e64.

Urban JH, Papenfort K, Thomsen J, Schmitz RA, Vogel J. 2007. A conserved small RNA promotes discoordinate expression of the *glmUS* operon mRNA to activate GlmS synthesis. *J Mol Biol* **373:** 521–528.

Vogel J, Luisi BF. 2011. Hfq and its constellation of RNA. *Nat Rev Microbiol* **9:** 578–589.

Xhemalce B, Robson SC, Kouzarides T. 2012. Human RNA methyltransferase BCDIN3D regulates MicroRNA processing. *Cell* **151:** 278–288.

Zisoulis DG, Kai ZS, Chang RK, Pasquinelli AE. 2012. Autoregulation of microRNA biogenesis by let-7 and Argonaute. *Nature* **486:** 541–544.